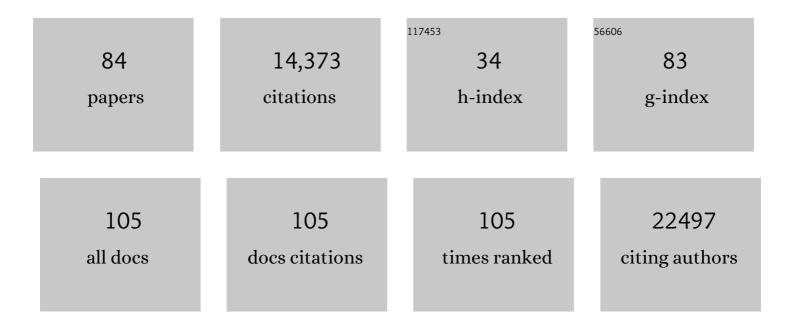
Ming Hu

List of Publications by Year in descending order

Source: https://exaly.com/author-pdf/7653832/publications.pdf Version: 2024-02-01



MINC HU

#	Article	IF	CITATIONS
1	Super interactive promoters provide insight into cell type-specific regulatory networks in blood lineage cell types. PLoS Genetics, 2022, 18, e1009984.	1.5	4
2	Understanding Regulatory Mechanisms of Brain Function and Disease through 3D Genome Organization. Genes, 2022, 13, 586.	1.0	7
3	THUNDER: A reference-free deconvolution method to infer cell type proportions from bulk Hi-C data. PLoS Genetics, 2022, 18, e1010102.	1.5	9
4	TWO-SIGMA-G: a new competitive gene set testing framework for scRNA-seq data accounting for inter-gene and cell–cell correlation. Briefings in Bioinformatics, 2022, 23, .	3.2	5
5	Mapping chromatin loops in single cells. Trends in Genetics, 2022, 38, 637-640.	2.9	9
6	A systematic evaluation of Hi-C data enhancement methods for enhancing PLAC-seq and HiChIP data. Briefings in Bioinformatics, 2022, 23, .	3.2	3
7	Predictive Assessment of Quantitative Ultra-Widefield Angiographic Features for Future Need for Anti-VEGF Therapy in Diabetic Eye Disease. Journal of Personalized Medicine, 2022, 12, 608.	1.1	2
8	SnapHiC2: A computationally efficient loop caller for single cell Hi-C data. Computational and Structural Biotechnology Journal, 2022, 20, 2778-2783.	1.9	7
9	The Association of Fluid Volatility With Subretinal Hyperreflective Material and Ellipsoid Zone Integrity in Neovascular AMD. , 2022, 63, 17.		7
10	Machine Learning–Based Automated Detection of Hydroxychloroquine Toxicity and Prediction of Future Toxicity Using Higher-Order OCT Biomarkers. Ophthalmology Retina, 2022, 6, 1241-1252.	1.2	6
11	Longitudinal panretinal microaneurysm dynamics on ultra-widefield fluorescein angiography in eyes treated with intravitreal aflibercept for proliferative diabetic retinopathy in the recovery study. British Journal of Ophthalmology, 2021, 105, 1111-1115.	2.1	11
12	Retinal Fluid Volatility Associated With Interval Tolerance and Visual Outcomes in Diabetic Macular Edema in the VISTA Phase III Trial. American Journal of Ophthalmology, 2021, 224, 217-227.	1.7	5
13	TWOâ€SICMA: A novel twoâ€component single cell modelâ€based association method for singleâ€cell RNAâ€sec data. Genetic Epidemiology, 2021, 45, 142-153.	0.6	11
14	Aqueous Cytokine Expression and Higher Order OCT Biomarkers: Assessment of the Anatomic-Biologic Bridge in the IMAGINE DME Study. American Journal of Ophthalmology, 2021, 222, 328-339.	1.7	24
15	FIREcaller: Detecting frequently interacting regions from Hi-C data. Computational and Structural Biotechnology Journal, 2021, 19, 355-362.	1.9	22
16	HiC-ACT: improved detection of chromatin interactions from Hi-C data via aggregated Cauchy test. American Journal of Human Genetics, 2021, 108, 257-268.	2.6	17
17	Longitudinal Assessment of Ellipsoid Zone Integrity, Subretinal Hyperreflective Material, and Subretinal Pigment Epithelium Disease in Neovascular Age-Related Macular Degeneration. Ophthalmology Retina, 2021, 5, 1204-1213.	1.2	28
18	Longitudinal Higher-Order OCT Assessment of Quantitative Fluid Dynamics and the Total Retinal Fluid Index in Neovascular AMD. Translational Vision Science and Technology, 2021, 10, 29.	1.1	15

Мімс Ни

#	Article	IF	CITATIONS
19	CTCF mediates dosage- and sequence-context-dependent transcriptional insulation by forming local chromatin domains. Nature Genetics, 2021, 53, 1064-1074.	9.4	90
20	MUNIn: A statistical framework for identifying long-range chromatin interactions from multiple samples. Human Genetics and Genomics Advances, 2021, 2, 100036.	1.0	0
21	Exploring the angiographic-biologic phenotype in the IMAGINE study: quantitative UWFA and cytokine expression. British Journal of Ophthalmology, 2021, , bjophthalmol-2020-318726.	2.1	4
22	Determining and forecasting drought susceptibility in southwestern Iran using multi-criteria decision-making (MCDM) coupled with CA-Markov model. Science of the Total Environment, 2021, 781, 146703.	3.9	55
23	SnapHiC: a computational pipeline to identify chromatin loops from single-cell Hi-C data. Nature Methods, 2021, 18, 1056-1059.	9.0	46
24	HPRep: Quantifying Reproducibility in HiChIP and PLAC-Seq Datasets. Current Issues in Molecular Biology, 2021, 43, 1156-1170.	1.0	4
25	Parallel characterization of cis-regulatory elements for multiple genes using CRISPRpath. Science Advances, 2021, 7, eabi4360.	4.7	16
26	Characterization of Ultra-Widefield Angiographic Vascular Features in Diabetic Retinopathy with Automated Severity Classification. Ophthalmology Science, 2021, 1, 100049.	1.0	4
27	Spatial heterogeneity modeling of water quality based on random forest regression and model interpretation. Environmental Research, 2021, 202, 111660.	3.7	75
28	Proximity Ligation-Assisted ChIP-Seq (PLAC-Seq). Methods in Molecular Biology, 2021, 2351, 181-199.	0.4	6
29	Promoter-proximal CTCF binding promotes distal enhancer-dependent gene activation. Nature Structural and Molecular Biology, 2021, 28, 152-161.	3.6	172
30	The 2-Year Leakage Index and Quantitative Microaneurysm Results of the RECOVERY Study: Quantitative Ultra-Widefield Findings in Proliferative Diabetic Retinopathy Treated with Intravitreal Aflibercept. Journal of Personalized Medicine, 2021, 11, 1126.	1.1	4
31	Transcriptional network orchestrating regional patterning of cortical progenitors. Proceedings of the United States of America, 2021, 118, .	3.3	25
32	Repeatability of automated leakage quantification and microaneurysm identification utilising an analysis platform for ultra-widefield fluorescein angiography. British Journal of Ophthalmology, 2020, 104, 500-503.	2.1	16
33	Quantitative Ultra-Widefield Angiographic Features and Associations with Diabetic Macular Edema. Ophthalmology Retina, 2020, 4, 49-56.	1.2	19
34	Longitudinal Panretinal Leakage and Ischemic Indices in Retinal Vascular Disease after Aflibercept Therapy. Ophthalmology Retina, 2020, 4, 154-163.	1.2	19
35	IMPACT OF OPTICAL COHERENCE TOMOGRAPHY ANGIOGRAPHY REVIEW STRATEGY ON DETECTION OF CHOROIDAL NEOVASCULARIZATION. Retina, 2020, 40, 672-678.	1.0	8
36	Cell-type-specific 3D epigenomes in the developing human cortex. Nature, 2020, 587, 644-649.	13.7	110

Мімс Ни

#	Article	IF	CITATIONS
37	RETINAL LEAKAGE INDEX DYNAMICS ON ULTRA-WIDEFIELD FLUORESCEIN ANGIOGRAPHY IN EYES TREATED WITH INTRAVITREAL AFLIBERCEPT FOR PROLIFERATIVE DIABETIC RETINOPATHY IN THE RECOVERY STUDY. Retina, 2020, 40, 2175-2183.	1.0	10
38	Global analysis of histone modifications and long-range chromatin interactions revealed the differential cistrome changes and novel transcriptional players in human dilated cardiomyopathy. Journal of Molecular and Cellular Cardiology, 2020, 145, 30-42.	0.9	11
39	Quantitative Analysis of Ellipsoid Zone in Acute Posterior Multifocal Placoid Pigment Epitheliopathy. Journal of Vitreoretinal Diseases, 2020, 4, 192-201.	0.2	2
40	Robust Hi-C Maps of Enhancer-Promoter Interactions Reveal the Function of Non-coding Genome in Neural Development and Diseases. Molecular Cell, 2020, 79, 521-534.e15.	4.5	110
41	Inferring Spatial Organization of Individual Topologically Associated Domains via Piecewise Helical Model. IEEE/ACM Transactions on Computational Biology and Bioinformatics, 2019, 17, 1-1.	1.9	1
42	Altered chromatin recruitment by FOXA1 mutations promotes androgen independence and prostate cancer progression. Cell Research, 2019, 29, 773-775.	5.7	20
43	Optical coherence tomography angiography characteristics of choroidal neovascularization requiring varied dosing frequencies in treat-and-extend management: An analysis of the AVATAR study. PLoS ONE, 2019, 14, e0218889.	1.1	14
44	Higher-Order Assessment of OCT in Diabetic Macular Edema from the VISTA Study: Ellipsoid Zone Dynamics and the Retinal Fluid Index. Ophthalmology Retina, 2019, 3, 1056-1066.	1.2	44
45	Quantitative Ultra-Widefield Angiography and Diabetic Retinopathy Severity. Ophthalmology, 2019, 126, 1527-1532.	2.5	71
46	A general result on complete convergence for weighted sums of linear processes and its statistical applications. Statistics, 2019, 53, 903-920.	0.3	8
47	Sensory experience remodels genome architecture in neural circuit to drive motor learning. Nature, 2019, 569, 708-713.	13.7	66
48	Joint analyses of multi-tissue Hi-C and eQTL data demonstrate close spatial proximity between eQTLs and their target genes. BMC Genetics, 2019, 20, 43.	2.7	20
49	MAPS: Model-based analysis of long-range chromatin interactions from PLAC-seq and HiChIP experiments. PLoS Computational Biology, 2019, 15, e1006982.	1.5	94
50	Predictive Model for Macular Hole Closure Speed: Insights From Intraoperative Optical Coherence Tomography. Translational Vision Science and Technology, 2019, 8, 18.	1.1	23
51	A Bayesian mixture model for clustering droplet-based single-cell transcriptomic data from population studies. Nature Communications, 2019, 10, 1649.	5.8	56
52	Common DNA sequence variation influences 3-dimensional conformation of the human genome. Genome Biology, 2019, 20, 255.	3.8	65
53	Circular ecDNA promotes accessible chromatin and high oncogene expression. Nature, 2019, 575, 699-703.	13.7	343
54	An ultra high-throughput method for single-cell joint analysis of open chromatin and transcriptome. Nature Structural and Molecular Biology, 2019, 26, 1063-1070.	3.6	239

Мілс Ни

#	Article	IF	CITATIONS
55	Quantitative assessment of outer retinal layers and ellipsoid zone mapping in hydroxychloroquine retinopathy. British Journal of Ophthalmology, 2019, 103, 3-7.	2.1	20
56	Transcriptomic and Protein Analysis of Small-cell Bladder Cancer (SCBC) Identifies Prognostic Biomarkers and DLL3 as a Relevant Therapeutic Target. Clinical Cancer Research, 2019, 25, 210-221.	3.2	48
57	Enhancing Hi-C data resolution with deep convolutional neural network HiCPlus. Nature Communications, 2018, 9, 750.	5.8	132
58	Histone H3 lysine 4 monomethylation modulates long-range chromatin interactions at enhancers. Cell Research, 2018, 28, 204-220.	5.7	131
59	Genome-wide association analyses identify 44 risk variants and refine the genetic architecture of major depression. Nature Genetics, 2018, 50, 668-681.	9.4	2,224
60	DIMM-SC: a Dirichlet mixture model for clustering droplet-based single cell transcriptomic data. Bioinformatics, 2018, 34, 139-146.	1.8	68
61	Integrative functional genomic analysis of human brain development and neuropsychiatric risks. Science, 2018, 362, .	6.0	516
62	The 3D Genome Browser: a web-based browser for visualizing 3D genome organization and long-range chromatin interactions. Genome Biology, 2018, 19, 151.	3.8	393
63	Assessment of inner and outer retinal layer metrics on the Cirrus HD-OCT Platform in normal eyes. PLoS ONE, 2018, 13, e0203324.	1.1	18
64	Gene regulation in the 3D genome. Human Molecular Genetics, 2018, 27, R228-R233.	1.4	61
65	Automated quantitative characterisation of retinal vascular leakage and microaneurysms in ultra-widefield fluorescein angiography. British Journal of Ophthalmology, 2017, 101, 696-699.	2.1	58
66	HUGIn: Hi-C Unifying Genomic Interrogator. Bioinformatics, 2017, 33, 3793-3795.	1.8	69
67	Polycomb-Mediated Disruption of an Androgen Receptor Feedback Loop Drives Castration-Resistant Prostate Cancer. Cancer Research, 2017, 77, 412-422.	0.4	23
68	LAIT: a local ancestry inference toolkit. BMC Genetics, 2017, 18, 83.	2.7	5
69	FastHiC: a fast and accurate algorithm to detect long-range chromosomal interactions from Hi-C data. Bioinformatics, 2016, 32, 2692-2695.	1.8	40
70	Genome-wide mapping and analysis of chromosome architecture. Nature Reviews Molecular Cell Biology, 2016, 17, 743-755.	16.1	324
71	The International Human Epigenome Consortium: A Blueprint for Scientific Collaboration and Discovery. Cell, 2016, 167, 1145-1149.	13.5	404
72	A Compendium of Chromatin Contact Maps Reveals Spatially Active Regions in the Human Genome. Cell Reports, 2016, 17, 2042-2059.	2.9	745

Ming Hu

#	Article	IF	CITATIONS
73	HiView: an integrative genome browser to leverage Hi-C results for the interpretation of GWAS variants. BMC Research Notes, 2016, 9, 159.	0.6	10
74	Emergency Department–Initiated Palliative Care in Advanced Cancer. JAMA Oncology, 2016, 2, 591.	3.4	194
75	Statistical Challenges in Analyzing Methylation and Long-Range Chromosomal Interaction Data. Statistics in Biosciences, 2016, 8, 284-309.	0.6	9
76	A hidden Markov random field-based Bayesian method for the detection of long-range chromosomal interactions in Hi-C data. Bioinformatics, 2016, 32, 650-656.	1.8	47
77	Widespread Rearrangement of 3D Chromatin Organization Underlies Polycomb-Mediated Stress-Induced Silencing. Molecular Cell, 2015, 58, 216-231.	4.5	299
78	The Distribution of Genomic Variations in Human iPSCs Is Related to Replication-Timing Reorganization during Reprogramming. Cell Reports, 2014, 7, 70-78.	2.9	24
79	Understanding spatial organizations of chromosomes via statistical analysis of Hi data. Quantitative Biology, 2013, 1, 156-174.	0.3	29
80	Bayesian Inference of Spatial Organizations of Chromosomes. PLoS Computational Biology, 2013, 9, e1002893.	1.5	188
81	Using Poisson mixed-effects model to quantify transcript-level gene expression in RNA-Seq. Bioinformatics, 2012, 28, 63-68.	1.8	29
82	HiCNorm: removing biases in Hi-C data via Poisson regression. Bioinformatics, 2012, 28, 3131-3133.	1.8	228
83	Topological domains in mammalian genomes identified by analysis of chromatin interactions. Nature, 2012, 485, 376-380.	13.7	5,786
84	HPeak: an HMM-based algorithm for defining read-enriched regions in ChIP-Seq data. BMC Bioinformatics, 2010, 11, 369.	1.2	94